

Structure of ionic liquids and concentrated electrolytes from a mesoscopic theory

A. Ciach

Institute of Physical Chemistry, Polish Academy of Sciences, 01-224 Warszawa, Poland

O. Patsahan

*Institute for Condensed Matter Physics of the National
Academy of Sciences of Ukraine, Lviv, Ukraine*

(Dated: November 7, 2022)

Abstract

Recently, underscreening in concentrated electrolytes was discovered in experiments and confirmed in simulations and theory. It was found that the correlation length of the charge-charge correlations, λ_s , satisfies the scaling relation $\lambda_s/\lambda_D \sim (a/\lambda_D)^n$, where λ_D is the Debye screening length and a is the ionic diameter. However, different values of n were found in different studies. In this work we solve this puzzle within the mesoscopic theory that yielded $n=3$ in agreement with experiments, but only very high densities of ions were considered [A. Ciach A. and O. Patsahan, *J.Phys.: Condens. Matter* **33**, 37LT01 (2021)]. Here we apply the theory to a broader range of density of ions and find that different values of n in the above scaling can yield a fair approximation for λ_s/λ_D for different ranges of a/λ_D . The experimentally found scaling holds for $2 < a/\lambda_D < 4$, and we find $n=3$ for the same range of the reduced Debye length. For smaller a/λ_D , we find $n=2$ obtained earlier in several simulation and theoretical studies, and still closer to the Kirkwood line we obtain $n=1.5$ that was also predicted in different works. It follows from our theory that $n=3$ (i.e. λ_s is proportional to the density of ions) when the variance of the local charge density is large, and λ_s is proportional to this variance times the Bjerrum length. Detailed derivation of the theory is presented.

I. INTRODUCTION

An interesting feature of ionic liquids and concentrated electrolytes is the hyperuniformity, meaning that the variance of the charge inside a region with the linear size R grows with R as R^{d-1} rather than as R^d for $R \gg a$, where d is the spacial dimension, and a is the diameter of the ions [1]. These small charge fluctuations indicate significant deviations from random distribution of the ions, and follow from the charge-neutrality condition. For this reason, concentrated electrolytes and ionic liquids (IL) can be viewed as a charge-neutral background for test charges. This picture is a sort of a 'negative' of dilute electrolytes. Instead of ions screening the test charge in dilute systems, in concentrated electrolytes we need 'holes', i.e. vacancies or solvent molecules violating the charge neutrality of the surroundings to screen the test charge. The screening length λ_s increases when the number of charge carries - ions in dilute and holes in concentrated electrolytes - decreases. Because the density of 'holes' decreases with increasing density of ions ρ , the screening length in concentrated electrolytes should increase with increasing ρ . This intuitive, qualitative picture was confirmed by experiments [2–4], simulations [5], and theory [6, 7].

In the experimental works [2–4] it was observed that the decay length of the disjoining pressure between crossed mica cylinders confining concentrated electrolytes was $\lambda_s/\lambda_D \sim (a/\lambda_D)^n$ with $n = 3$, where

$$\lambda_D = \sqrt{\frac{k_B T \epsilon}{4\pi e^2 \rho}} \quad (1)$$

is the Debye screening length with ϵ , e , k_B and T denoting the dielectric constant, charge, the Boltzmann constant and temperature, respectively. The same scaling relation was observed for several different systems, including alkali halide solutions, pure ionic liquids and ionic liquid solutions. This effect has been termed as underscreening.

A similar scaling should be obeyed by the correlation length in the bulk electrolyte. Indeed, the experimentally observed scaling was predicted in Ref. [7] for the restricted primitive model (RPM) of hard spheres with equal diameters and equal magnitude of the charge in a structureless solvent. In Ref. [7], the RPM was studied within the mesoscopic theory for inhomogeneous systems [8, 9]. However, only very high densities of ions were considered in Ref. [7], because the assumptions allowing for obtaining analytical results in this theory are valid only when the charge-density waves with the wavelength $\sim 2a$ (nearest-neighbors oppositely charged) appear with a high probability, which is the case for high densities of

ions. It was shown that in such conditions, λ_s is proportional to a variance of the charge in regions with the size $\sim a$. In different theories and simulations, $n = 3$ was not found. Rather, n in the range $1 < n \leq 2$ was obtained in the scaling relation $\lambda_s/\lambda_D \sim (a/\lambda_D)^n$ [5, 6, 10–18]. It is very difficult to achieve equilibrium in simulations of concentrated electrolytes at low T , and very long simulation runs are required. Finite size effects and noise make it difficult to observe and interpret the correlations at large distances. The results were thus obtained for not so large ρ and not so low T .

The issue of underscreening is still under active debates. Recent atomic force spectroscopy measurements for electrolyte solutions complemented by classical density functional theory calculations for the primitive model did not demonstrate a large increase in decay length with increasing salt concentration [19]. Alternatively, underscreening found previously in experiments for concentrated electrolytes [2–4] and obtained within the mesoscopic theory for the RPM [7] has been also found in very recent simulations for the RPM and supported by applying a minimal cluster theory [20].

In this work we extend the studies of ref. [7] to a broader range of ionic densities and temperature. As the assumptions allowing for analytical results are not valid for small and medium densities of ions, here we solve our self-consistent equations for the correlation function numerically. In Sec. II we consider the variance of the local charge in dilute and concentrated electrolytes. To highlight the role of the variance of the charge in regions with the size comparable with a in concentrated electrolytes, we present a simplified model and estimate the correlation length for the charge correlations. In Sec. III we present the formalism of the mesoscopic theory applied to RPM. The results are presented in Sec. IV A for the charge-charge correlations and in Sec. IV B for the density-density correlations. Our results are compared with experiment, simulations and other theoretical results. The last section V contains our conclusions.

II. VARIANCE OF A LOCAL CHARGE IN DILUTE AND CONCENTRATED ELECTROLYTES - QUALITATIVE CONSIDERATIONS

In contrast to the small variance of the charge in regions with $R \gg a$, the variance of the charge in a subsystem with $R < 2a$ is large if the electrolyte is concentrated. As illustrated in Fig. 1, in dilute electrolytes any small subsystem contains typically solvent molecules

and is therefore uncharged in majority of the microscopic states. However, the larger is the density of ions, the more often a subsystem with $R < 2a$ is occupied either by an anion or by a cation. Occupancy of the small subsystem by a half of the anion and a half of the cation is rare. Thus, even though the average charge is zero, the variance of the local charge grows with the density of ions and in concentrated electrolytes becomes large. When the local charge density in the majority of the microscopic states is different from the average charge density, then the fluctuations of the local charge density play an important role and cannot be neglected. In particular, the properly calculated average energy can be significantly different from the energy calculated for the average (vanishing) charge density. The variance of the local charge density is the main difference between dilute and concentrated electrolytes and ionic liquids (IL). While fluctuations of the local charge density can be neglected in the former case, they have to be taken into account in concentrated electrolytes and IL or IL solutions.

In order to analyze the effect of the large variance of the local charge density on the properties of ionic systems, let us consider a local deviation $\phi(\mathbf{r}) = c(\mathbf{r}) - c$ of the charge density from the average value c , and its variance $\langle \phi^2 \rangle$. The dimensionless charge density in the case of the same valency of the anions and the cations is given by

$$c(\mathbf{r}) = \rho_+(\mathbf{r}) - \rho_-(\mathbf{r}), \quad (2)$$

with $\rho_+(\mathbf{r})$ and $\rho_-(\mathbf{r})$ denoting the dimensionless local density of the cations and the anions. The local dimensionless number density of the ions is defined by

$$\rho(\mathbf{r}) = \rho_+(\mathbf{r}) + \rho_-(\mathbf{r}). \quad (3)$$

In a macroscopic system, $\rho_i = a^3 N_i / V$, with $i = +, -$, and N_i denoting the number of i -th type ions inside the macroscopic volume V . The local density should be defined in a somewhat different way, because the mesoscopic volume can be occupied by a fraction of an ion (see Fig. 1). Thus, we define the local densities by $\rho_i(\mathbf{r}) = 6\zeta_i(\mathbf{r})/\pi$, where $\zeta_i(\mathbf{r})$ is the fraction of the mesoscopic volume around \mathbf{r} that is occupied by the ion of the i -th type. The construction of ζ_i is illustrated in Fig. 2. We assume that the charge e is uniformly distributed over the volume of the ion, and $ec(\mathbf{r})$ is a continuous charge density. In the disordered phase and in absence of any boundaries or external fields, $\langle c \rangle = 0$ and $\langle \phi^2 \rangle$ is position independent.

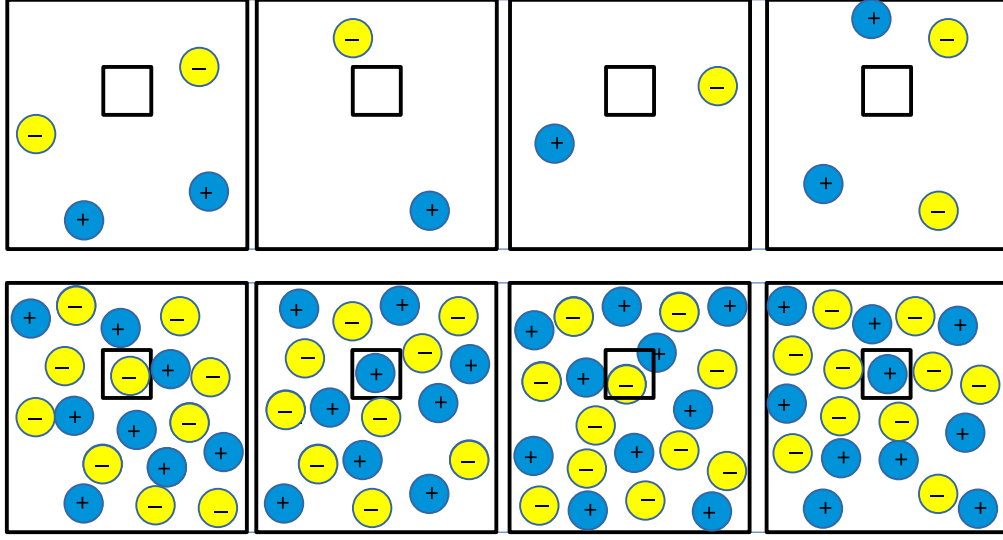


FIG. 1: Cartoon showing microstates of ions in dilute (top row) and concentrated (bottom row) electrolytes. The solvent molecules are not shown for clarity. The small square inside the system represents a mesoscopic subsystem. In the dilute electrolyte the subsystem is typically uncharged, while in the concentrated one, very often either an anion or a cation is present inside it. The considered subsystem is therefore either negatively or positively charged, even though the charge averaged over all microstates vanishes. The variance of the charge, however, in the bottom row is large.

Let us divide the system into cells with the linear size $a \leq R < 2a$. We expect that in concentrated electrolytes the standard deviation of the charge from zero in each cell is equal to $+\sqrt{\langle\phi^2\rangle}$ or $-\sqrt{\langle\phi^2\rangle}$. A representative distribution of the positive and negative sign of $\sqrt{\langle\phi^2\rangle}$ among the cells in our simplified model of a concentrated electrolyte is shown in Fig.3. The distribution of the + and - sign among the cells is governed by the competition between the entropy favoring the random distribution of the signs, and the energy favoring oppositely charged neighbors. Let us focus on the two distinguished cells in Fig. 3 separated by the distance $r^* = r/a$. We shall measure the distance in a -units in the whole article, but the asterisk will be omitted for clarity of the notation. There are four possible pairs of signs in these two cells, $[+,+]$, $[-,-]$, $[+,-]$ and $[-,+]$. If we require that the selected cells are oppositely charged, the internal energy in $k_B T$ units decreases by $-l_B \langle\phi^2\rangle/r$ where

$$l_B = \frac{e^2}{k_B T \epsilon a} = \frac{1}{4\pi\rho\lambda_D^2 a} \quad (4)$$

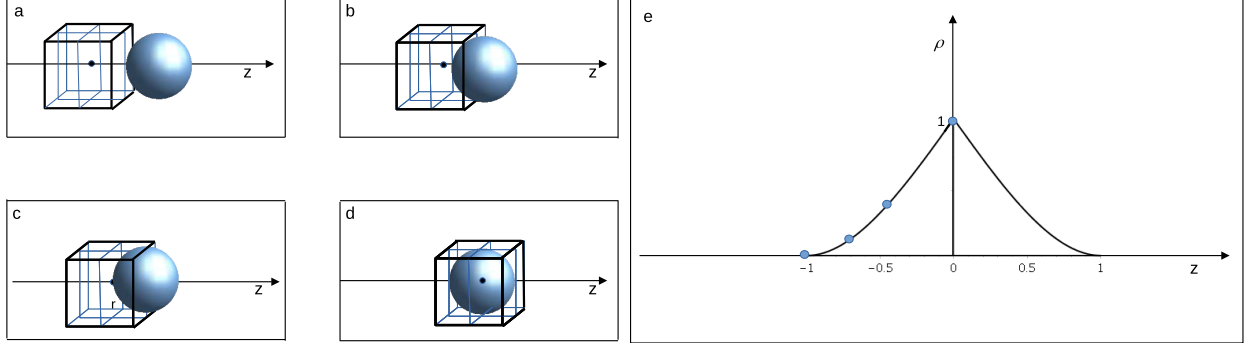


FIG. 2: Illustration of the mesoscopic density for a single sphere with the diameter $a = 1$ and the center at $\mathbf{r} = (0, 0, 0)$. The mesoscopic region is represented by the cube with the edge of the length 1 and the center shown as the black circle at $\mathbf{r} = (0, 0, -1), (0, 0, -0.75), (0, 0, -0.5), (0, 0, 0)$ in panels a, b, c and d, respectively. The mesoscopic density $\rho = 6\zeta/\pi$, with ζ representing the fraction of the volume of the cube that is occupied by the particles, is shown in panel (e) as a function of z , with the blue circles referring to the illustrations in panels a-d.

is the Bjerrum length, i.e. the distance between the ions at which the Coulomb potential equals the thermal energy $k_B T$, in a -units.

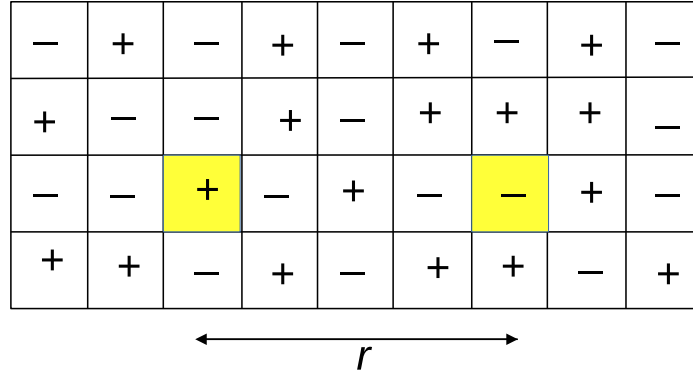


FIG. 3: The concentrated electrolyte or IL divided into cells with the size $a \leq R < 2a$, and a representative distribution of the sign of the standard deviation of the local charge from zero, $\pm\sqrt{\langle\phi^2\rangle}$. If we require that the selected cells separated by the distance r are oppositely charged, then both the energy and the entropy of the system decrease, giving negative or positive excess free energy for r smaller or larger than $l_B\langle\phi^2\rangle/\ln 2$, respectively.

The decrease of the energy is accompanied by a decrease of the entropy - two less states of the two cells are possible - and the excess free energy associated with fixing opposite charges in the cells separated by the distance r is

$$\beta\Delta F \approx \frac{-l_B\langle\phi^2\rangle}{r} + \ln 2, \quad (5)$$

where $\beta = 1/(k_B T)$. We can easily see that $\beta\Delta F < 0$ for $r < l_B\langle\phi^2\rangle/\ln 2$, and the energy wins, while for distances larger than $l_B\langle\phi^2\rangle/\ln 2$ the entropy dominates. It is thus favourable to correlate the charges up to the distance $r \propto l_B\langle\phi^2\rangle$. This distance can be considered as a rough estimation of the correlation length for the charge-charge correlations. In large systems the variance of the fluctuating quantity is proportional to the number of the fluctuating objects, therefore we conclude that the correlation length λ_S should be approximately proportional to $l_B\rho$. However, the estimation $l_B\langle\phi^2\rangle \propto l_B\rho$ cannot be exact for the considered mesoscopic regions, especially when ρ is not large.

In the mean-field (MF) approximation, the average quantities such as the internal energy, are calculated on the basis of average densities of the components. MF works very well when in majority of the microscopic states the local densities are equal or close to the average densities. In the case of a large variance of the local densities, however, the energy in a large number of the microscopic states can be significantly different from the energy in the microstates with the densities equal or close to the average densities. In this case the averaging of the energy with the appropriate probability distribution can lead to a result quite different from the energy calculated for the average densities. For the remaining average quantities, including correlation at large distances, similar strong effect of the variance of the local densities can be expected. Thus, the fluctuation contribution to the grand thermodynamic potential should be taken into account in all the systems with large variance of the local densities.

III. MATHEMATICAL FORMALISM OF THE MESOSCOPIC THEORY FOR ELECTROLYTES AND IL

In this section we summarize the formalism developed in a series of works and applied to different systems with competing interactions [8, 9, 21, 22]. We consider the mesoscopic densities ρ_i discussed in the previous section that for the ionic systems are more convenient

than the local volume fractions, but in fact differ from the latter only by the factor $6/\pi$. A particular form of $\rho_i(\mathbf{r})$ can be induced by external fields $h_i(\mathbf{r})$, and the grand potential functional of h_i can be written in the form

$$\beta\Omega_h[\{h_i\}] = -\ln \int D\rho_+ \int D\rho_- \exp\left(-\beta\Omega_{co}[\{\rho_i\}] + \beta \int d\mathbf{r} h_i(\mathbf{r})\rho_i(\mathbf{r})\right). \quad (6)$$

The summation convention for repeated indexes is used here and below. In (6), the integration over the mesoscopic degrees of freedom, ρ_i , and the integration over the microscopic states for each fixed ρ_i are performed separately. $\exp(-\beta\Omega_{co}[\{\rho_i\}])$ is equal to $\exp(-\beta H)$ integrated over all the microscopic states compatible with given ρ_i , with H denoting the microscopic Hamiltonian. Because $\Omega_{co}[\{\rho_i\}]$ is calculated for fixed ρ_i , i.e. with suppressed mesoscopic fluctuations, we can use the MF approximation for it. According to the general thermodynamic formula,

$$\Omega_{co}[\{\rho_i\}] = U_{co}[\{\rho_i\}] - TS_{co}[\{\rho_i\}] - \mu \int d\mathbf{r} \rho(\mathbf{r}), \quad (7)$$

where $U_{co}[\{\rho_i\}]$ and $S_{co}[\{\rho_i\}]$ are the internal energy and the entropy, respectively, in the presence of the constraints $\{\rho_i\}$ imposed on the microscopic states, and μ is the chemical potential of the ions. We assume $-TS_{co} = \int d\mathbf{r} f_h(\rho_+(\mathbf{r}), \rho_-(\mathbf{r}))$, where

$$\beta f_h = \rho_+ \ln \rho_+ + \rho_- \ln \rho_- + \beta f_{ex}(\rho) \quad (8)$$

is the free-energy per unit volume of the hard-core reference system in the local-density approximation. The first two terms come from the entropy of mixing, and the last term describes packing of hard cores. For the internal energy we postulate

$$U_{co}[\{\rho_i\}] = \frac{1}{2} \int d\mathbf{r}_1 \int d\mathbf{r} \rho_i(\mathbf{r}_1) V_{ij}(r) g_{ij}(r) \rho_j(\mathbf{r}_1 + \mathbf{r}), \quad (9)$$

where $r = |\mathbf{r}|$ and $V_{ij}(r)$ is the interaction between the ions of the i -th and j -th type, and $g_{ij}(r)$ is the pair distribution function. In general, the interaction potential consists of the Coulomb potential and possible additional interactions. In the case of suppressed mesoscopic fluctuations, we assume $g_{ij}(r) = \theta(r - 1)$, where θ is the unit step function, and r is in a -units. With this assumption, we avoid contributions to the internal energy from overlapping hard cores of the ions, and have $g_{ij}(r) = 1$ for $r \rightarrow \infty$. If only the Coulomb potential is taken into account, then we obtain the simple formula

$$\beta U_{co} = \frac{l_B}{2} \int d\mathbf{r}_1 \int d\mathbf{r} c(\mathbf{r}_1) \frac{\theta(r - 1)}{r} c(\mathbf{r}_1 + \mathbf{r}) = \frac{l_B}{2} \int \frac{d\mathbf{k}}{(2\pi)^3} \frac{4\pi \cos k}{k^2} \hat{c}(\mathbf{k}) \hat{c}(-\mathbf{k}), \quad (10)$$

where $\hat{c}(\mathbf{k})$ denotes the function c in Fourier representation, and $k = |\mathbf{k}|$. We will use the same convention (a hat) for all functions in Fourier representation in the 3 dimensional space.

Once the form of Ω_{co} is assumed, we can return to the generating functional of the correlation functions, (6). The average mesoscopic density at \mathbf{r} , and the correlation function between fluctuations of ρ_i in the mesoscopic regions around \mathbf{r}_1 and \mathbf{r}_2 are given by

$$\bar{\rho}_i(\mathbf{r}) = \frac{\delta(-\beta\Omega_h)}{\delta(\beta h_i(\mathbf{r}))} \quad (11)$$

and

$$G_{ij}(\mathbf{r}_1 - \mathbf{r}_2) = \langle \rho_i(\mathbf{r}_1) \rho_j(\mathbf{r}_2) \rangle - \bar{\rho}_i(\mathbf{r}_1) \bar{\rho}_j(\mathbf{r}_2) = \frac{\delta \bar{\rho}_i(\mathbf{r}_1)}{\delta \beta h_j(\mathbf{r}_2)}. \quad (12)$$

The Legendre transform

$$\beta\Omega[\{\bar{\rho}_i\}] = \beta\Omega_h[\{h_i\}] + \beta \int d\mathbf{r} h_i(\mathbf{r}) \bar{\rho}_i(\mathbf{r}) \quad (13)$$

is a functional of $\bar{\rho}_i$, generating the inverse correlation functions,

$$C_{ij}(\mathbf{r}_1 - \mathbf{r}_2) = \frac{\delta^2 \beta\Omega}{\delta \bar{\rho}_i(\mathbf{r}_1) \delta \bar{\rho}_j(\mathbf{r}_2)} = \frac{\delta \beta h_i(\mathbf{r}_1)}{\delta \bar{\rho}_j(\mathbf{r}_2)}. \quad (14)$$

From (12) and (14) one can easily get the analog of the Ornstein-Zernike (OZ) equation, namely $\mathbf{G} = \mathbf{C}^{-1}$ in the matrix sense.

Using (6), we write the functional (13) in the form

$$\beta\Omega[\{\bar{\rho}_i\}] = \beta\Omega_{co}[\{\bar{\rho}_i\}] - \ln \int D\phi_+ \int D\phi_- \exp \left(-\beta H_f[\{\bar{\rho}_i, \phi_i\}] \right) \quad (15)$$

where $\phi_i(\mathbf{r}) = \rho_i(\mathbf{r}) - \bar{\rho}_i$ is the local fluctuation of ρ_i , and

$$\beta H_f[\{\bar{\rho}_i, \phi_i\}] = \beta\Omega_{co}[\{\bar{\rho}_i + \phi_i\}] - \beta\Omega_{co}[\{\bar{\rho}_i\}] - \beta \int d\mathbf{r} h_i(\mathbf{r}) \phi_i(\mathbf{r}). \quad (16)$$

The probability that the local fluctuations ϕ_i appear is proportional to $\exp(-\beta H_f)$, and the correlation functions can be obtained from the formula

$$G_{ij}(\mathbf{r}_1, \mathbf{r}_2) = \langle \phi_i(\mathbf{r}_1) \phi_j(\mathbf{r}_2) \rangle = \frac{\int D\phi_+ \int D\phi_- e^{-\beta H_f} \phi_i(\mathbf{r}_1) \phi_j(\mathbf{r}_2)}{\int D\phi_+ \int D\phi_- e^{-\beta H_f}}. \quad (17)$$

It is difficult to calculate the correlation functions from (12) or (17), unless we make some approximations. In order to develop such an approximate theory, we focus on C_{ij} . As follows from (15) and (14), the matrix \mathbf{C} contains a contribution from $\beta\Omega_{co}$ associated

with microscopic fluctuations (the first term in (15)), and the contribution associated with the mesoscopic fluctuations $\phi_i(\mathbf{r})$ (the second term in (15)), and is given by the following expression

$$C_{ij}(r) = \frac{\delta^2(\beta\Omega_{co})}{\delta\bar{\rho}_i(\mathbf{r}_1)\delta\bar{\rho}_j(\mathbf{r}_1 + \mathbf{r})} + \left\langle \frac{\delta^2(\beta H_f)}{\delta\bar{\rho}_i(\mathbf{r}_1)\delta\bar{\rho}_j(\mathbf{r}_1 + \mathbf{r})} - \frac{\delta(\beta H_f)}{\delta\bar{\rho}_i(\mathbf{r}_1)} \frac{\delta(\beta H_f)}{\delta\bar{\rho}_j(\mathbf{r}_1 + \mathbf{r})} \right\rangle \quad (18)$$

In this equation, the inverse correlation function is expressed in terms of the average of a function of ϕ_+, ϕ_- that can be expanded in a series of correlations of different orders.

In the fully symmetrical case, it is convenient to calculate the charge-charge and the density-density correlations, $G_{cc}(r) = \langle c(\mathbf{r}_1)c(\mathbf{r}_1 + \mathbf{r}) \rangle$ and $G_{\rho\rho}(r) = \langle \rho(\mathbf{r}_1)\rho(\mathbf{r}_1 + \mathbf{r}) \rangle - \bar{\rho}^2$, because $C_{c\rho} = 0$ for $\bar{c} = 0$ (vanishing external fields). In addition, from the considerations in the previous section it follows that we should take into account the variance of the local charge density. We shall limit ourselves to two-point correlation functions in (18), and make the self-consistent Gaussian approximation

$$\beta H_f[\{\bar{\rho}_i, \phi_i\}] \approx \beta H_G[\bar{c}, \bar{\rho}, \phi, \psi] \quad (19)$$

with $\phi = c - \bar{c}, \psi = \rho - \bar{\rho}$ and

$$\beta H_G[\bar{c}, \bar{\rho}, \phi, \psi] = \frac{1}{2} \int d\mathbf{r}_1 \int d\mathbf{r}_2 (\phi(\mathbf{r}_1)C_{cc}(r)\phi(\mathbf{r}_2) + \psi(\mathbf{r}_1)C_{\rho\rho}(r)\psi(\mathbf{r}_2)), \quad (20)$$

where $C_{\alpha\beta}$ with $\alpha, \beta = c, \rho$ is a functional of $\bar{c}, \bar{\rho}$ satisfying an equation analogous to Eq.(18). In principle, the term proportional to $C_{c\rho}$ should be included in (20). However, we neglect this term along with the other neglected terms in $H_f - H_G$, since for $\bar{c} = 0$ this term vanishes. We stress that H_G is not equal to the Taylor expansion of H_f truncated at the second order term if the fluctuation contribution in (18) is present.

In the Gaussian approximation (19)-(20), we have

$$\begin{aligned} C_{cc}(r) &= \frac{\delta^2\beta\Omega}{\delta c(\mathbf{r}_1)\delta c(\mathbf{r}_1 + \mathbf{r})} \\ &= \frac{\delta^2(\beta\Omega_{co})}{\delta c(\mathbf{r}_1)\delta c(\mathbf{r}_1 + \mathbf{r})} + \left\langle \frac{\delta^2(\beta H_G)}{\delta c(\mathbf{r}_1)\delta c(\mathbf{r}_1 + \mathbf{r})} - \frac{\delta(\beta H_G)}{\delta c(\mathbf{r}_1)} \frac{\delta(\beta H_G)}{\delta c(\mathbf{r}_1 + \mathbf{r})} \right\rangle \end{aligned} \quad (21)$$

with analogous equation for $C_{\rho\rho}$. In order to solve (21) and (20) self-consistently, we assume that the fluctuation contribution to the two-point functions should be taken into account according to Eq.(21), but for the higher-order functional derivatives of $\beta\Omega$ (i.e. the functional derivatives of $C_{\alpha\alpha}$), the fluctuation contribution in (15) and (21) can be disregarded. This

approximation for $C_{\alpha\alpha}$ corresponds to the self-consistent one-loop approximation in the field-theoretic approach. Based on this assumption, we make for $n + m > 2$ the approximation

$$\frac{\delta^{n+m}(\beta\Omega)}{\delta c(\mathbf{r}_1)\dots\delta c(\mathbf{r}_n)\delta\rho(\mathbf{r}_{n+1})\dots\delta\rho(\mathbf{r}_{n+m})} \approx \frac{\delta^{n+m}(\beta\Omega_{co})}{\delta c(\mathbf{r}_1)\dots\delta c(\mathbf{r}_n)\delta\rho(\mathbf{r}_{n+1})\dots\delta\rho(\mathbf{r}_{n+m})}. \quad (22)$$

In the local density approximation for $\beta f_h(\{\rho_i\})$, we have for $n + m > 2$

$$\frac{\delta^{n+m}(\beta\Omega_{co})}{\delta c(\mathbf{r}_1)\dots\delta c(\mathbf{r}_n)\delta\rho(\mathbf{r}_{n+1})\dots\delta\rho(\mathbf{r}_{n+m})} = A_{m,n}(c, \rho)\delta(\mathbf{r}_1 - \mathbf{r}_2)\dots\delta(\mathbf{r}_{n+m-1} - \mathbf{r}_{n+m}) \quad (23)$$

where

$$A_{m,n}(c, \rho) = \frac{\partial^{n+m}(\beta f_h)}{\partial^n c \partial^m \rho}. \quad (24)$$

It is convenient to consider the correlation functions in Fourier representation, because $C_{cp} = 0$ for $\bar{c} = 0$, and for G_{cc} and $G_{\rho\rho}$ defined by an equation analogous to (17) we have $\hat{G}_{cc}(k) = 1/\hat{C}_{cc}(k)$ and $\hat{G}_{\rho\rho}(k) = 1/\hat{C}_{\rho\rho}(k)$. Note that the product of the Coulomb potential and $\theta(r - 1)$ in Fourier representation is $4\pi \cos k/k^2$ that takes a negative minimum for $k_0 \approx 2.46$. Thus, charge waves with the wavelength $2\pi/k_0$ are energetically favored. This means that neighboring regions with the charge larger and smaller from zero occur with a high probability, and the variance of the local charge,

$$\langle\phi^2\rangle = \int \frac{d\mathbf{k}}{(2\pi)^3} \hat{C}_{cc}^{-1}(k) \quad (25)$$

should be taken into account, as already argued in sec.II. Local fluctuations of ρ are not energetically favored (see (9) and Fig.1), large local density fluctuation are not expected. Thus, $\langle\psi^2\rangle$ can be neglected. With the above assumptions, the equations for the inverse correlation functions in the self-consistent Gaussian approximation take the forms

$$\hat{C}_{cc}(k) \approx \frac{4\pi l_B \cos k}{k^2} + A_{0,2} + \frac{A_{0,4}}{2} \langle\phi^2\rangle \quad (26)$$

with $\langle\phi^2\rangle$ given in (25), and

$$\hat{C}_{\rho\rho}(k) \approx A_{2,0} + \frac{A_{2,2}}{2} \langle\phi^2\rangle + \beta \hat{V}_{fl}(k), \quad (27)$$

where

$$\beta \hat{V}_{fl}(k) = -\frac{A_{1,2}^2}{2} \int d\mathbf{r} e^{i\mathbf{k}\cdot\mathbf{r}} G_{cc}(r)^2 - \frac{A_{3,0}^2}{2} \int d\mathbf{r} e^{i\mathbf{k}\cdot\mathbf{r}} G_{\rho\rho}(r)^2. \quad (28)$$

We took into account that in the Gaussian approximation, $\langle\phi^2(\mathbf{r}_1)\phi^2(\mathbf{r}_2)\rangle = 2\langle\phi(\mathbf{r}_1)\phi(\mathbf{r}_2)\rangle^2$. Note that $A_{m,n}$ depends only on the entropy of mixing for $n > 0$, therefore $\hat{C}_{cc}(k)$ does

not depend on our approximation for the free energy density associated with the packing of ions. On the other hand, $\hat{C}_{\rho\rho}(k)$ depends on this approximation through $A_{2,0}$ and $A_{3,0}$, therefore we expect that $\hat{G}_{\rho\rho}(k)$ depends on the geometry of ions more strongly than the charge-charge correlations.

Self-consistent solutions of (25)-(28) together with $\hat{C}_{cc}(k) = 1/\hat{G}_{cc}(k)$ and $\hat{C}_{\rho\rho}(k) = 1/\hat{G}_{\rho\rho}(k)$ give us the correlation functions. We should note, however that the integral in Eq.(25) must be cutoff regularized. The accuracy in this theory is limited by the cutoff dependence of $\langle\phi^2\rangle$, but according to the construction of the mesoscopic theory, the cutoff Λ is not a free parameter. The wavelengths of the charge density are limited from below because the hard cores cannot overlap, and the nearest neighbors should be oppositely charged in the charge-waves that occur with sufficiently high-probability. We assume that consistent with the scale of coarse-graining set by the diameter of the ion, the cutoff in (25) should belong to a rather narrow range of values around $\Lambda \approx 2\pi/2 = \pi$. As we show in the next section, the dependence on Λ decreases with increasing $l_B\rho$.

IV. PROPERTIES OF THE CORRELATION FUNCTIONS

A. Asymptotic decay of charge-charge correlations

In order to determine the charge-charge correlations for different parts of the phase diagram, we use (24) for $A_{m,n}$ and write (26) in the form

$$\hat{C}_{cc}(k) \approx \frac{4\pi l_B \cos k}{k^2} + \frac{1}{\rho_R}, \quad (29)$$

where we introduced the "renormalized density" ρ_R that satisfies the self-consistent equation (see (24)-(26))

$$\frac{1}{\rho_R} = \frac{1}{\rho} + \frac{1}{\rho^3} \int_0^\Lambda \frac{dk}{(2\pi)^2} \frac{2k^2}{4\pi l_B \cos k/k^2 + 1/\rho_R}. \quad (30)$$

We assume $\Lambda = \pi$ and solve (30) numerically. The charge-charge correlations for $\hat{C}_{cc}(k)$ given by (29) were calculated in Ref. [23], but with ρ_R in (29) simply equal to ρ , i.e. with neglected fluctuations. We can use the results of Ref. [23] if we replace ρ by ρ_R obtained from the solution of (30).

According to the standard pole analysis, we have

$$G_{cc}(r) = \frac{1}{2\pi r} \sum_n \frac{e^{iq_n r} q_n}{\hat{C}'_{cc}(q_n)}, \quad (31)$$

where q_n are simple poles with positive imaginary parts of \hat{G}_{cc} extended to the complex q -plane, and $\hat{C}'_{cc}(q_n)$ is the derivative at $q = q_n$. The poles of $\hat{G}_{cc}(q)$ satisfy the equation

$$\frac{4\pi \cos q}{q^2} + S^R = 0 \quad (32)$$

where $S^R = 1/(\rho_R l_B)$, and the relevant poles are $q = i\alpha_0 \pm \alpha_1$, where $1/\alpha_0$ is equal to the correlation length λ_s , and α_1 is the wave number of the oscillations. For $S^R > S_K^R \approx 11.8$, there are two imaginary poles that satisfy the equation

$$\frac{4\pi \cosh \alpha_0}{\alpha_0^2} = S^R, \quad (33)$$

and the monotonic asymptotic decay of correlations is determined by the smaller solution of (33). The two imaginary poles coalesce at the Kirkwood line $S^R = S_K^R \approx 11.8$, and the inverse decay length at this line satisfies $\tanh \alpha_K = 2/\alpha_K$. For $S^R < S_K^R$ there is a pair of complex poles $q_{1,2} = i\alpha_0 \pm \alpha_1$, and

$$G_{cc}(r) = A_c e^{-\alpha_0 r} \sin(\alpha_1 r + \theta)/r. \quad (34)$$

We should note that in this mesoscopic theory, the microscopic structure is smeared out (see Fig. 2), and we can only predict the decay of correlations at large distances.

We determine the Kirkwood line by a numerical solution of the equation (see (30))

$$S^R = \frac{1}{\rho l_B} + \frac{1}{(\rho l_B)^2 \rho} \int_0^\pi \frac{dk}{(2\pi)^2} \frac{2k^2}{4\pi \cos k/k^2 + S^R} \quad (35)$$

for $S^R = 11.8$. In Fig. 4, $1/l_B$ at the Kirkwood line is shown as a function of ρ together with our MF and mean spherical approximation results as well as with simulation results, $a/\lambda_D \approx 1.37$, obtained in Ref. [15]. Although we only expect a semi-quantitative accuracy of the cutoff-dependent result, the agreement with the simulations results is rather good for $\Lambda = \pi$, but our result deviates a little from a straight line.

When the fluctuation contribution to $\hat{C}_{cc}(k)$ is neglected, then $\hat{G}_{cc}(k)$ diverges for $k = k_0 \approx 2.46$ at the λ -line given by $(\rho_R l_B)^{-1} = |4\pi \cos k_0/k_0^2| \approx 1.61$. However, when the fluctuation contribution is included, the resulting equation (see (35))

$$|4\pi \cos k_0/k_0^2| = \frac{1}{\rho l_B} + \frac{1}{(\rho l_B)^2 \rho} \int_0^\Lambda \frac{dk}{(2\pi)^2} \frac{2k^2}{4\pi \cos k/k^2 + |4\pi \cos k_0/k_0^2|} \quad (36)$$

has no solutions for $1/(\rho l_B) > 0$, because the integral diverges, and the instability line is shifted to $T = 0$, as already discussed in Ref. [25] in the context of ions and in the original

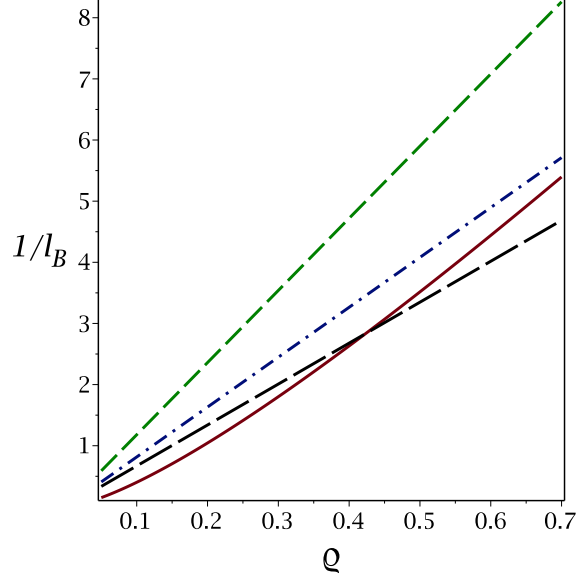


FIG. 4: Kirkwood line separating the monotonic and the oscillatory decay of charge-charge correlations with the fluctuation contribution to \hat{C}_{cc} neglected (green dashed line) and included (red solid line). Blue dash-dotted line shows the MSA result ($a/\lambda_D \approx 1.24$) [23, 24] and black long-dash line shows simulation result ($a/\lambda_D \approx 1.37$) [15]. ρ is the dimensionless density of ions, and the Bjerrum length l_B in units of the ion diameter a is inversely proportional to absolute temperature.

Brazovskii work [26] in the context of an order-parameter in the Landau-type theory for the order-disorder transition to an oscillatory state.

In Ref. [7], $\hat{C}_{cc}(k)$ was approximated by

$$\hat{C}_{cc}(k) \approx \hat{C}_a(k) = \hat{C}_{cc}(k_0) + \beta v(k^2 - k_0^2)^2, \quad (37)$$

obtained from a truncated Taylor expansion about the minimum at $k = k_0$, modified by the requirement that the approximation for $\hat{C}_{cc}(k)$ should be an even function of k . Next it was argued that for relatively small values of S^R corresponding to large ρl_B , the cutoff-regularized integral can be approximated by

$$\int_0^\pi \frac{dk}{(2\pi)^2} \frac{2k^2}{\hat{C}_{cc}(k)} \approx \int_0^\infty \frac{dk}{(2\pi)^2} \frac{2k^2}{\hat{C}_a(k)}, \quad (38)$$

because in the case of a pronounced maximum of $\hat{G}_{cc}(k)$ at $k = k_0$, the main contribution to the integral comes from the vicinity of k_0 , and

$$\int_\pi^\infty \frac{dk}{(2\pi)^2} \frac{2k^2}{\hat{C}_a(k)} \ll \int_0^\pi \frac{dk}{(2\pi)^2} \frac{2k^2}{\hat{C}_a(k)}. \quad (39)$$

The advantage of the approximation (38) is the possibility of analytical calculation of the integral on the RHS of Eq. (38) and analytical solution of the corresponding approximate form of (26) and (25). As can be seen in Fig. 5, the integral on the RHS of Eq. (38) differs significantly from the integral on the LHS of Eq. (38) at the Kirkwood line, and in general for large values of S^R , because the contribution to the integral from $k > \pi$ is large compared to the contribution from $k < \pi$. For small S^R , however, in particular for $S^R = 1.7$ shown in Fig. 5, the contribution to the integral $\int_0^\infty \frac{dk}{(2\pi)^2} \frac{2k^2}{\hat{C}_a(k)}$ from $k > \pi$ is much smaller from the contribution from $k < \pi$. Thus, we can use the approximate expression (37) for $\hat{C}_{cc}(k)$ only in the region of the phase diagram limited to rather small S^R , i.e. to large densities and Bjerrum lengths. Under the assumption of large $l_B\rho$, the variance of the local charge

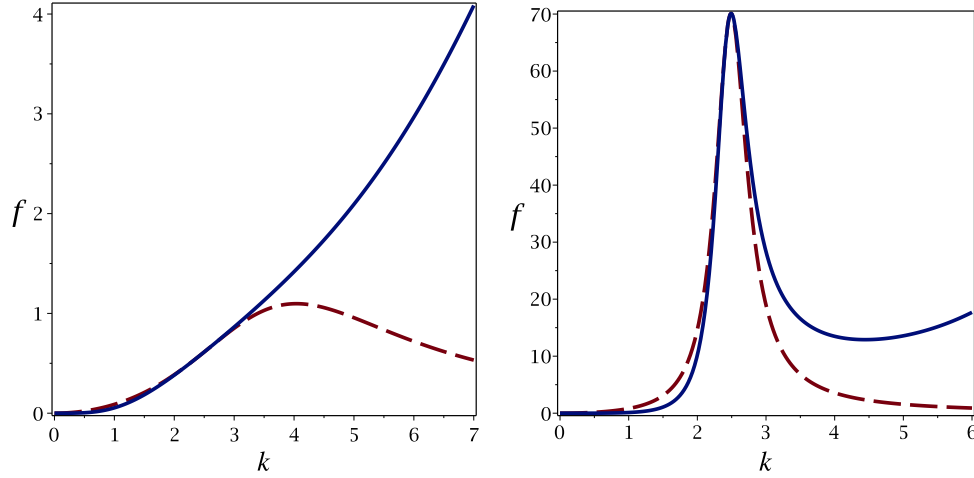


FIG. 5: The integrands, $f(k) = 2k^2/\hat{C}_{cc}(k)$ (solid line), and $f(k) = 2k^2/\hat{C}_a(k)$ (dashed line), on the LHS and the RHS in Eq. (38), respectively. Left panel: at the Kirkwood line ($S^R = 11.8$). Right panel: for $S^R = 1.7$ with S^R defined in (35).

density takes the form [7]

$$\langle \phi^2 \rangle \approx \frac{k_0}{4\pi \sqrt{\tilde{C}_{cc}(k_0) \beta v}}. \quad (40)$$

$\tilde{C}_{cc}(k_0)$ is obtained by the self-consistent solution of (26) and (40). The parameters in (34) are $A_c \approx \langle \phi^2 \rangle / k_0$, $\alpha_1 \approx k_0$ and

$$\alpha_0^{-1} \approx 8\pi\beta v \langle \phi^2 \rangle \approx 1.1 l_B \langle \phi^2 \rangle. \quad (41)$$

The proportionality of the decay length to $l_B \langle \phi^2 \rangle$ agrees with our heuristic analysis of concentrated electrolytes. Moreover, both the analytical results and our heuristic arguments

are valid only when ρl_B is large.

For a broader range of ρl_B we determine α_0 numerically. In Fig. 6, the decay length α_0^{-1} is shown as a function of ρl_B for fixed ρ and fixed l_B , in particular, the results are given for $\rho = 0.4, 0.7$ and for $l_B = 2.3, 4.6$. Although in this theory α_0 depends on a single thermodynamic parameter S^R (see (32)), S^R depends on ρ and l_B separately (see (35)). For the fixed dimensionless densities of ions ρ , α_0^{-1} depends on $l_B \rho$ almost linearly for $\rho l_B > 1.5$, but the slope increases with ρ . For the fixed Bjerrum lengths l_B , α_0^{-1} also increases almost linearly with $l_B \rho$ but it occurs for larger ρl_B and the slope decreases when l_B increases. It turns out that our analytical solution underestimates a little the correlation length α_0^{-1} , but the lines $\alpha_0^{-1}(l_B)$ obtained with and without the approximation (37) are almost parallel, and shifted with respect to each other by ~ 0.5 (see Fig. 7).

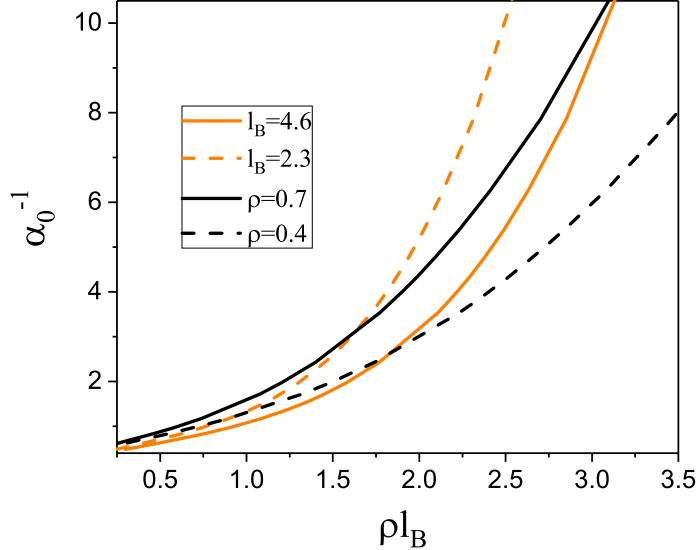


FIG. 6: The correlation length of the oscillatory decay of the charge-charge correlations, α_0^{-1} , as a function of ρl_B for the fixed dimensionless density of ions ρ and for the fixed Bjerrum length l_B as it is given in the legend. l_B is in units of the ion diameter a .

Figure 8 (left panel) shows the ratio of the charge-charge decay length to the Debye length, α_0^{-1}/λ_D , as a function of the inverse of the Debye length, a/λ_D (in log-log scale). The results are given for the same values of fixed ρ and l_B as in Fig. 6. Using these results, we test the scaling relation $\alpha_0^{-1}/\lambda_D \sim (a/\lambda_D)^n$. Our analysis revealed the existence of different scaling regimes corresponding to different values of n . In particular, we found that $n = 3$ for the range $2.5 < a/\lambda_D < 4$, $n = 2$ for $1.5 < a/\lambda_D < 2.5$, and $n = 1.5$ for a/λ_D closer to

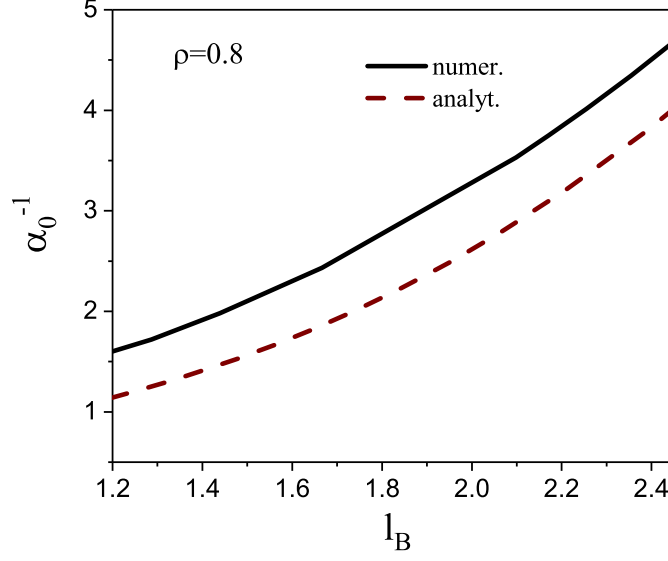


FIG. 7: The correlation length of the oscillatory decay of the charge-charge correlations α_0^{-1} as a function of the Bjerrum length l_B for the dimensionless density of ions $\rho = 0.8$ from the approximate analytical theory (bottom line) and with numerical solution of Eq. (30) (top line). l_B is in units of the ion diameter a .

the Kirkwood point. A typical picture of the scaling regimes is presented in Fig. 8 (right panel) for the case $\rho = 0.7$ (see Supplemental Material for details).

In Fig. 9, we present the comparison of the predictions of the mesoscopic theory with the experimental data for aqueous NaCl solutions [2]. As it is seen, we obtain a semiquantitative agreement with experimental findings for $2 < a/\lambda_D < 4$. Moreover, the agreement becomes quantitative if one assumes that the average diameter of hydrated ions in the experiment is equal to 0.67 nm.

B. Asymptotic decay of density-density correlations

When the fluctuation contribution is not included in (27), the density-density correlations are strictly short-range in our local-density approximation when the energy depends only on the charge density. The k -dependence of $\hat{C}_{\rho\rho}(k)$ comes from $\hat{V}_{fl}(k)$ that is induced by the correlations between fluctuations. $\hat{V}_{fl}(k)$ takes a negative minimum for $k = 0$ (see (28)), and for $k \rightarrow 0$ can be Taylor expanded. The Taylor expansion of $\hat{V}_{fl}(k)$ takes the same mathematical form as the Taylor expanded attractive interactions in Fourier representation,

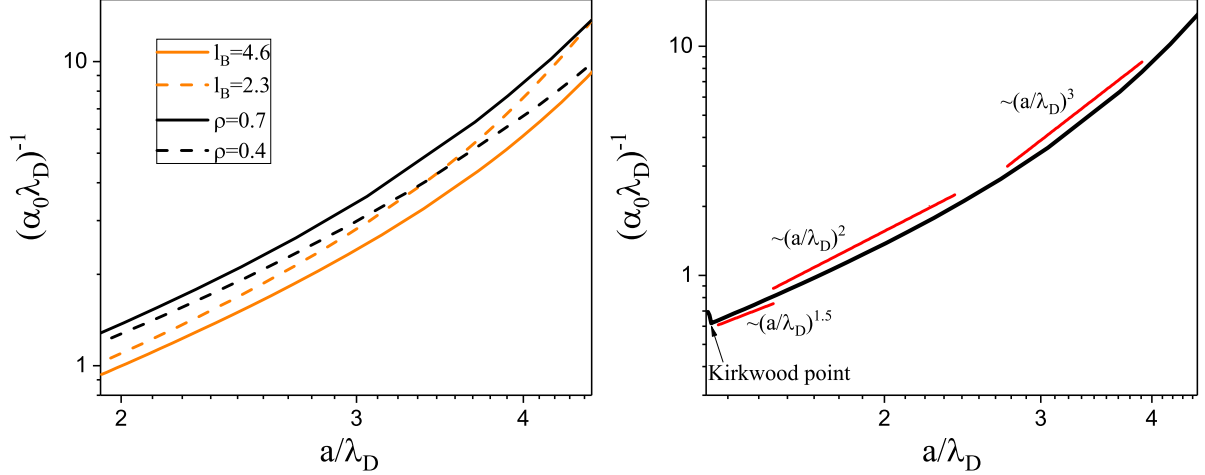


FIG. 8: Left panel: A double logarithmic plot of the ratio of the correlation length of the oscillatory decay of the charge-charge correlations and Debye length, $(\alpha_0\lambda_D)^{-1}$, as a function of the inverse of the Debye length, a/λ_D , for the dimensionless density of ions ρ and the Bjerrum length l_B as it is given in the legend. Right panel: the same as in the left panel for $\rho = 0.7$ with the indication of the regions where different scaling regimes hold. The arrow points to the cusp (Kirkwood point) where crossover from monotonic to oscillatory decay occurs.

and we have the approximation

$$\hat{C}_{\rho\rho}(k) = R_0 + R_2 k^2 + O(k^4). \quad (42)$$

The rather lengthy formulas for R_n can be found in Ref. [9] (Appendix A). From (42) we obtain the asymptotic decay in real space for $r \gg 1$,

$$G_{\rho\rho}(r) = \frac{1}{4\pi R_2} \frac{\exp(-r\sqrt{R_0/R_2})}{r}. \quad (43)$$

We can see that the asymptotic decay of the density-density correlations is monotonic, with the decay length $\xi_\rho = \sqrt{R_2/R_0}$ depending on the charge-charge correlations (see (28) and (27)). Explicit expressions for R_0, R_2 can be obtained by a self-consistent solution of (42), (27) and (28) with Taylor-expanded $\hat{V}_{fl}(k)$. $\hat{V}_{fl}(k)$ depends on the form of $G_{cc}(r)$ that except from large densities must be determined numerically, therefore the self-consistent solution of (42), (27) and (28) is obtained numerically too. We assume the Carnahan-Starling approximation [27],

$$\beta f_{ex}(\zeta) = \rho \left[\frac{4\zeta - 3\zeta^2}{(1 - \zeta)^2} - 1 \right], \quad (44)$$

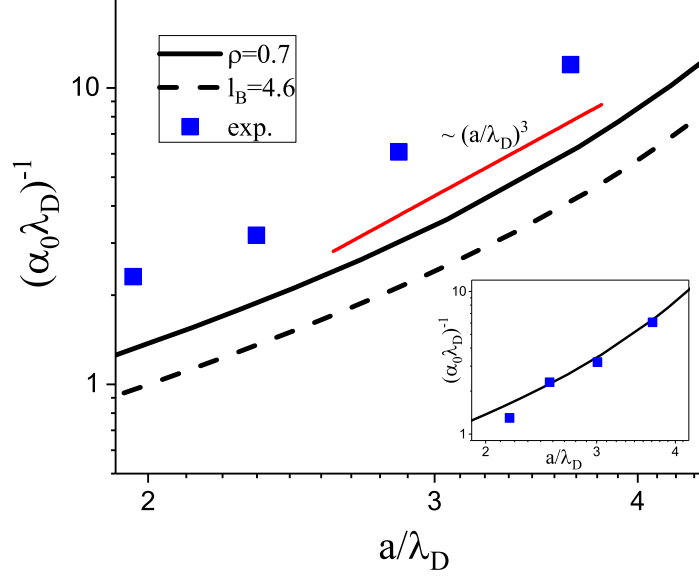


FIG. 9: A double logarithmic plot of the ratio α_0^{-1}/λ_D as a function of a/λ_D . The blue solid squares are the experimental results of Smith et al. [2] (Supporting Information) for NaCl in water for $a = 0.52$ nm (hydrated ions). The curves show the theoretical predictions for the dimensionless density of ions $\rho = 0.7$ (solid line) and for the Bjerrum length $l_B = 4.6$ (dashed line). The red solid line depicts power law as noted. l_B is in units of the ion diameter a . Inset: the same as in the main plot for $\rho = 0.7$, assuming that in the experiment the hydrated ion diameter was 0.67 nm.

with $\zeta = \pi\rho/6$, and show the resulting correlation length in Fig. 10 and in Fig. 11 for fixed ρ and l_B , respectively. In both figures, the left panel shows the dependence of the decay length ξ_ρ on ρl_B . In the right panel, we show the ratio ξ_ρ/λ_D as a function of the inverse of the Debye length a/λ_D in log-log scale. For both, the fixed ρ and the fixed l_B , ξ_ρ (ξ_ρ/λ_D) is an increasing function of ρl_B (a/λ_D) for $\rho l_B > 2$ ($a/\lambda_D > 5$) and its behaviour is nonmonotonic with a rather deep minimum for $\rho l_B \approx 2$ ($a/\lambda_D \approx 5$). Furthermore, ξ_ρ/λ_D increases as $(a/\lambda_D)^5$ for $a/\lambda_D > 5$. For $\rho l_B < 2$ ($a/\lambda_D < 5$), the behaviour of ξ_ρ for the fixed ρ and the fixed l_B is completely different. In this case, ξ_ρ (ξ_ρ/λ_D) decreases (increases) when ρl_B (a/λ_D) increases for the fixed dimensionless densities of ions $\rho = 0.4$ and $\rho = 0.6$. Interestingly, in this region ξ_ρ/λ_D increases linearly with a/λ_D . For the fixed Bjerrum lengths $l_B = 2.3$ and $l_B = 4.6$, ξ_ρ and ξ_ρ/λ_D shows a nonmonotonic behaviour with a maximum and the maximum is higher for $l_B = 2.3$. Simultaneously, for $l_B = 4.6$, both the maximum and the minimum are shifted to larger ρl_B (a/λ_D) when compared with $l_B = 2.3$.

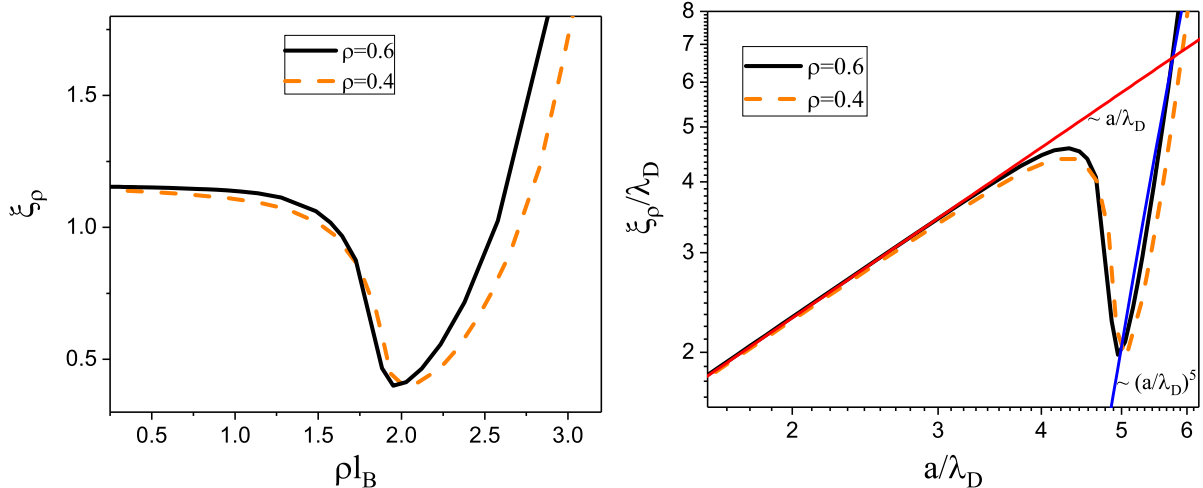


FIG. 10: Left panel: the decay length of the density-density correlations ξ_ρ as a function of ρl_B for the fixed dimensionless densities of ions $\rho = 0.4$ (dashed line) and $\rho = 0.6$ (solid line). l_B is in units of the ion diameter a . Right panel: a double logarithmic plot of the ratio of the decay length of the density-density correlation function and Debye length, ξ_ρ/λ_D , as a function of the inverse of the Debye length, a/λ_D , for the dimensionless densities of ions $\rho = 0.4$ (dashed line) and $\rho = 0.6$ (solid line). Red and blue solid lines depict power laws as noted.

V. CONCLUSIONS

We have found that the dependence of the correlation length in electrolytes on the density of ions and the Bjerrum length has a more complex behavior than just a simple scaling $\lambda_s/\lambda_D = \alpha_0^{-1}/\lambda_D \sim (a/\lambda_D)^n$. The above formula can be a fair approximation for the charge-charge correlation length, but with the exponent n taking different values for different ranges of a/λ_D . From our theory it follows that n increases with increasing a/λ_D . In particular, for the fixed dimensionless density of ions $\rho = 0.7$, we find $n = 3$ for the range $2.5 < a/\lambda_D < 4$, $n = 2$ for the range $1.5 < a/\lambda_D < 2.5$, and $n = 1.5$ for a/λ_D closer to the Kirkwood point. The existence of different scaling regimes for different ranges of a/λ_D was already reported in [17]. It should be noted that the scaling exponent $n \approx 2$ was found for the RPM theoretically [6], as well as in simulations [16, 18]. Moreover, the anomalous underscreening for the RPM that agrees with experimental results was obtained very recently in simulations and by theory accounting for ions pairing in Ref. [20].

We should note that $n = 3$ perfectly fits the experimental results for $a/\lambda_D > 2$, but for

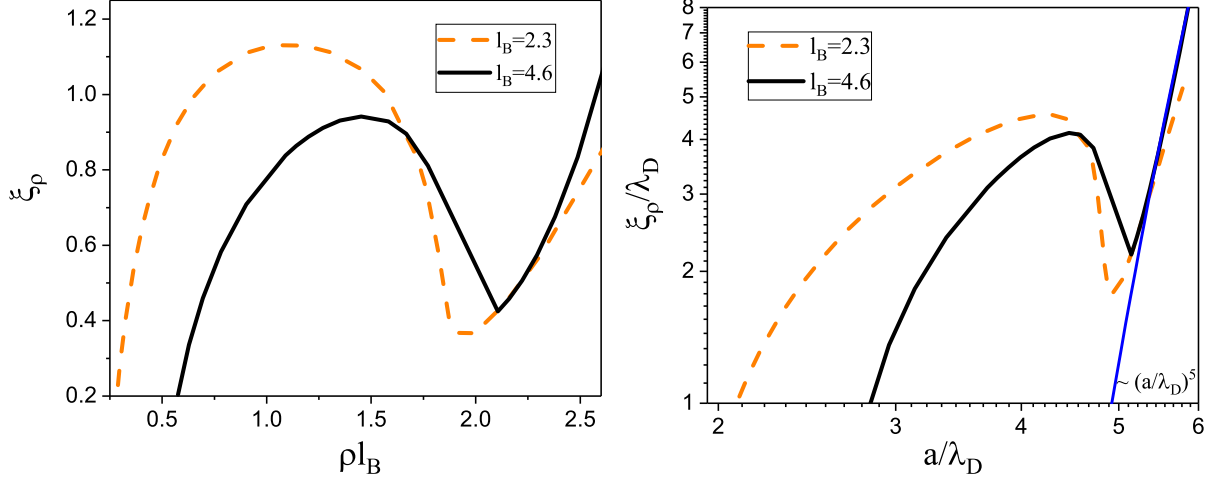


FIG. 11: Left panel: the decay length of the density-density correlations ξ_ρ as a function of ρl_B for the fixed Bjerrum lengths $l_B = 2.3$ and $l_B = 4.6$. l_B is in units of the ion diameter a . Right panel: a double logarithmic plot of the ratio of the decay length of the density-density correlations and Debye length, ξ_ρ/λ_D , as a function of the inverse of the Debye length, a/λ_D , for the Bjerrum lengths $l_B = 2.3$ (dashed line) and $l_B = 4.6$ (solid line). Blue solid line depicts a power law as noted.

$a/\lambda_D < 2$, the scaling $\lambda_s/\lambda_D \sim (a/\lambda_D)^3$ is less good. Notably, $n = 3$ corresponds to $\lambda_s \sim l_B \rho$. In our theory, we obtain $\lambda_s \sim l_B \langle \phi^2 \rangle$ for large $l_B \rho$, and the scaling $\lambda_s \sim l_B \rho$ is obtained when the variance of the local charge behaves as $\langle \phi^2 \rangle \propto \rho$, which is a rough approximation. The relation $\lambda_s \sim l_B \langle \phi^2 \rangle$ is also obtained from the very simplified lattice model, with the charge taking the value $\pm \sqrt{\langle \phi^2 \rangle}$ in the lattice cells with the lattice constant a . Both, the simplified model and our analytical theory are not valid for medium density of ions, and from numerical solution of our equations we obtain the exponent n in fair agreement with simulations and other theoretical results. We should also mention quite good agreement between the Kirkwood line obtained in our theory and in simulations [15]. We conclude that the results of our theory form a bridge between the experiment, simulations and other theoretical predictions.

In addition to the charge-charge correlation we study the density-density correlations. The obtained density-density correlation function decays monotonically. The corresponding asymptotic decay length ξ_ρ depends on the charge-charge correlations in addition to the correlations associated with the hard spheres (steric) interactions. This result significantly

differs from the results obtained previously for the decay length of the density-density correlation function which take into account only the contribution from the steric interactions [12, 15].

-
- [1] S. Torquato, *Physics Reports* **745**, 1 (2018).
 - [2] A. M. Smith, A. A. Lee, and S. Perkin, *J. Phys. Chem. Lett.* **7**, 2157 (2016).
 - [3] A. Lee, C. S. Perez-Martinez, A. M. Smith, and S. Perkin, *Phys. Rev. Lett.* **119**, 026002 (2017).
 - [4] T. S. Groves, C. S. Perez-Martinez, R. Lhermerout, and S. Perkin, *J. Phys. Chem. Lett.* **12**, 1702 (2021).
 - [5] J. Zeman, S. Kondrat, and C. Holm, *Chem. Comm.* **56**, 15635 (2020).
 - [6] R. M. Adar, S. A. Safran, H. Diamant, and D. Andelman, *Phys. Rev. E* **100**, 042615 (2019).
 - [7] A. Ciach and O. Patsahan, *J. Phys.: Condens. Matter* **33**, 37LT01 (2021).
 - [8] A. Ciach, *Phys. Rev. E* **78**, 061505 (2008).
 - [9] O. Patsahan, A. Meyra, and A. Ciach, *J. Mol. Liq.* **363**, 119844 (2022).
 - [10] Z. A. Goodwin and A. A. Kornyshev, *Electrochem. Commun.* **82**, 129 (2017).
 - [11] N. B. Ludwig, K. Dasbiswas, D. V. Talapin, and S. Vaikuntanathan, *J. Chem. Phys.* **149**, 164505 (2018).
 - [12] F. Coupette, A. A. Lee, and A. Härtel, *Phys. Rev. Lett.* **121** (2018).
 - [13] B. Rotenberg, O. Bernard, and J.-P. Hansen, *J. Phys.: Condens. Matter* **30**, 054005 (2018).
 - [14] S. W. Coles, C. Park, R. Nikam, M. Kanduč, J. Dzubiella, and B. Rotenberg, *J. Phys. Chem. B* **124**, 1778 (2020).
 - [15] P. Cats, R. Evans, A. Härtel, and R. van Roij, *J. Chem. Phys.* **154**, 124504 (2021).
 - [16] J. Zeman, S. Kondrat, and C. Holm, *J. Chem. Phys.* **155**, 204501 (2021).
 - [17] C. W. Outhwaite and L. B. Bhuiyan, *J. Chem. Phys.* **155**, 014504 (2021).
 - [18] E. Krucker-Velasquez and J. W. Swan, *J. Chem. Phys.* **155**, 134903 (2021).
 - [19] S. Kumar, P. Cats, M. B. Alotaibi, S. C. Ayirala, A. A. Yousef, R. van Roij, I. Siretanu, and F. Mugele, *Journal of Colloid and Interface Science* **622**, 819 (2022).
 - [20] A. Härtel, M. Bültmann, and F. Coupette, *Anomalous underscreening in the restricted primitive model* (2022), URL <https://arxiv.org/abs/2209.03486>.

- [21] A. Ciach, *Mol. Phys* **109**, 1101 (2011).
- [22] A. Ciach, *Soft Matter* **14**, 5497 (2018).
- [23] A. Ciach, W. T. Gózdź, and R. Evans, *J. Chem. Phys.* **118**, 3702 (2003).
- [24] C. Outhwaite, *Statistical mechanics. A Specialist periodic Report*, vol. 2 (The Chemical Society, London, 1975), p.188.
- [25] A. Ciach and G. Stell, *Int.J. Mod. Phys. B* **19**, 3309 (2005).
- [26] S. A. Brazovskii, *Sov. Phys. JETP* **41**, 85 (1975).
- [27] G. Mansoori, N. F. Carnahan, K. E. Starling, and J. T. W. Leland, *J. Chem. Phys.* **54**, 1523 (1971).